

Supplementary Data - Raman Spectroscopy and Group and Basis-Restricted Non Negative Matrix Factorisation Identifies Radiation Induced Metabolic Changes in Human Cancer Cells

Kirsty Milligan¹, Xincheng Deng¹, Phillip Shreeves², Ramie Ali-Adeeb¹, Quinn Matthews³, Alexandre Brolo⁴, Julian J. Lum^{5,6}, Jeffrey L. Andrews², and Andrew Jirasek^{1*}

¹Department of Physics, The University of British Columbia, Kelowna, Canada

²Department of Statistics, The University of British Columbia, Kelowna, Canada

³BC Cancer, Centre for the North, Prince George, Canada

⁴Department of Chemistry, University of Victoria, Victoria, Canada

⁵Department of Biochemistry and Microbiology, University of Victoria, Victoria, Canada

⁶Trev and Joyce Deeley Research Centre, BC Cancer, Victoria, Canada

*andrew.jirasek@ubc.ca

Table S1. 30-reference-biochemical Raman chemical library

Alanine
Arginine
Asparagine
Citric acid
CoEnzymeA
Cysteine
DNA
Glucose
Glutamic acid
Glutathione
Glycerol
Glyceryl tripalmitoleate
Glycogen
Histidine
Isoleucine
Lactose
Mannose
Methionine
Oleic acid
Palmitic acid
Phenylalanine
Phosphatidylcholine
Phosphatidylserine
Phosphatidylinositol
Serine
Stearic acid
Triglycerides
Tryptophan
Tyrosine
Valine

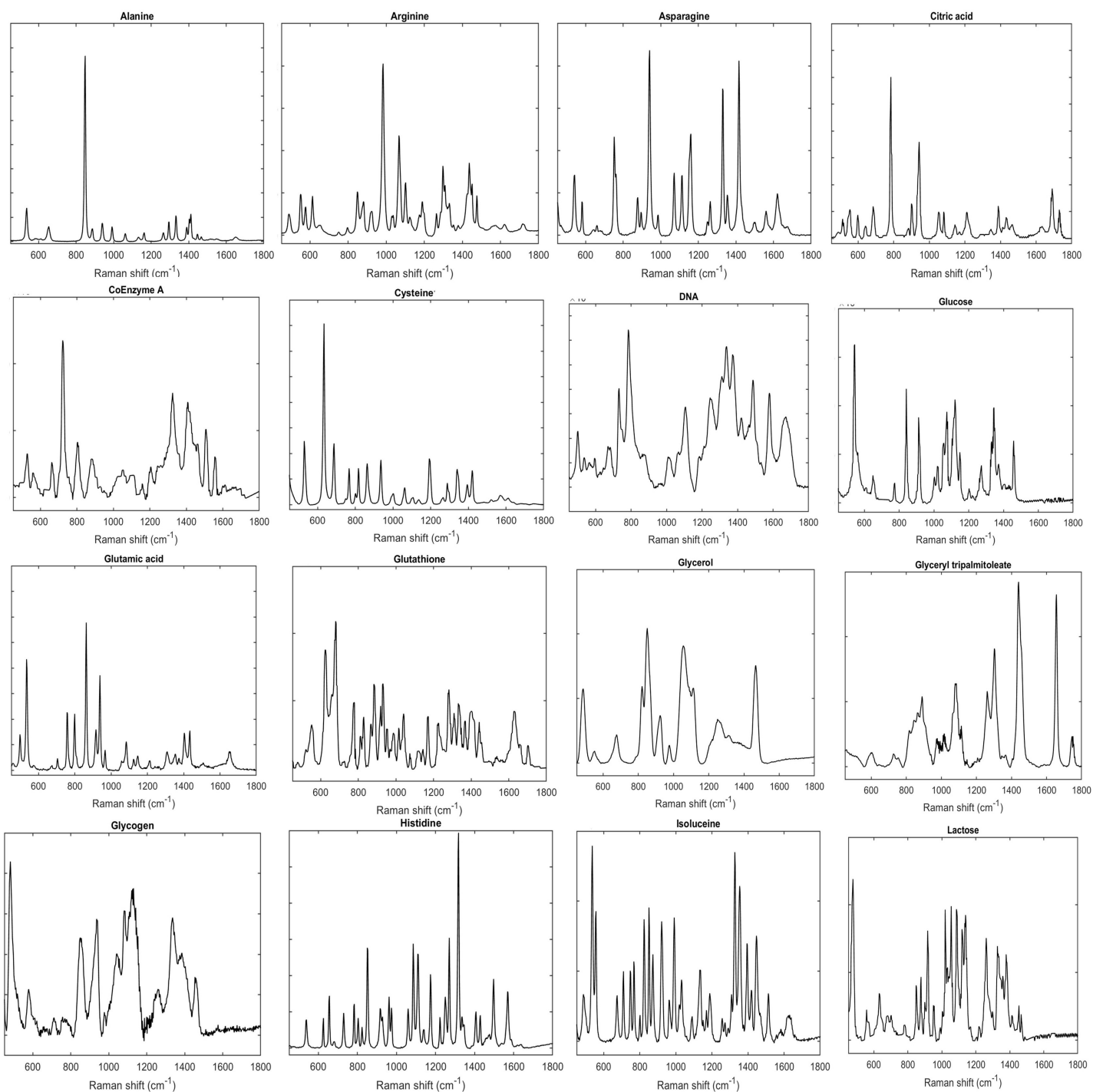


Figure S1. Raman spectra of biochemicals 1-16 as listed in table S1 which were used in the GBR-NMF model. All spectra were acquired using a Renishaw InVia system (dry 100x objective), using an excitation wavelength of 785 nm. Spectra were collected from biochemicals in their pure form. All spectra have been baseline corrected and smoothed using standard Savitsky-Golay filtering algorithms in MatLab. The spectra were then normalised such that the area under the curve was equal to 1.

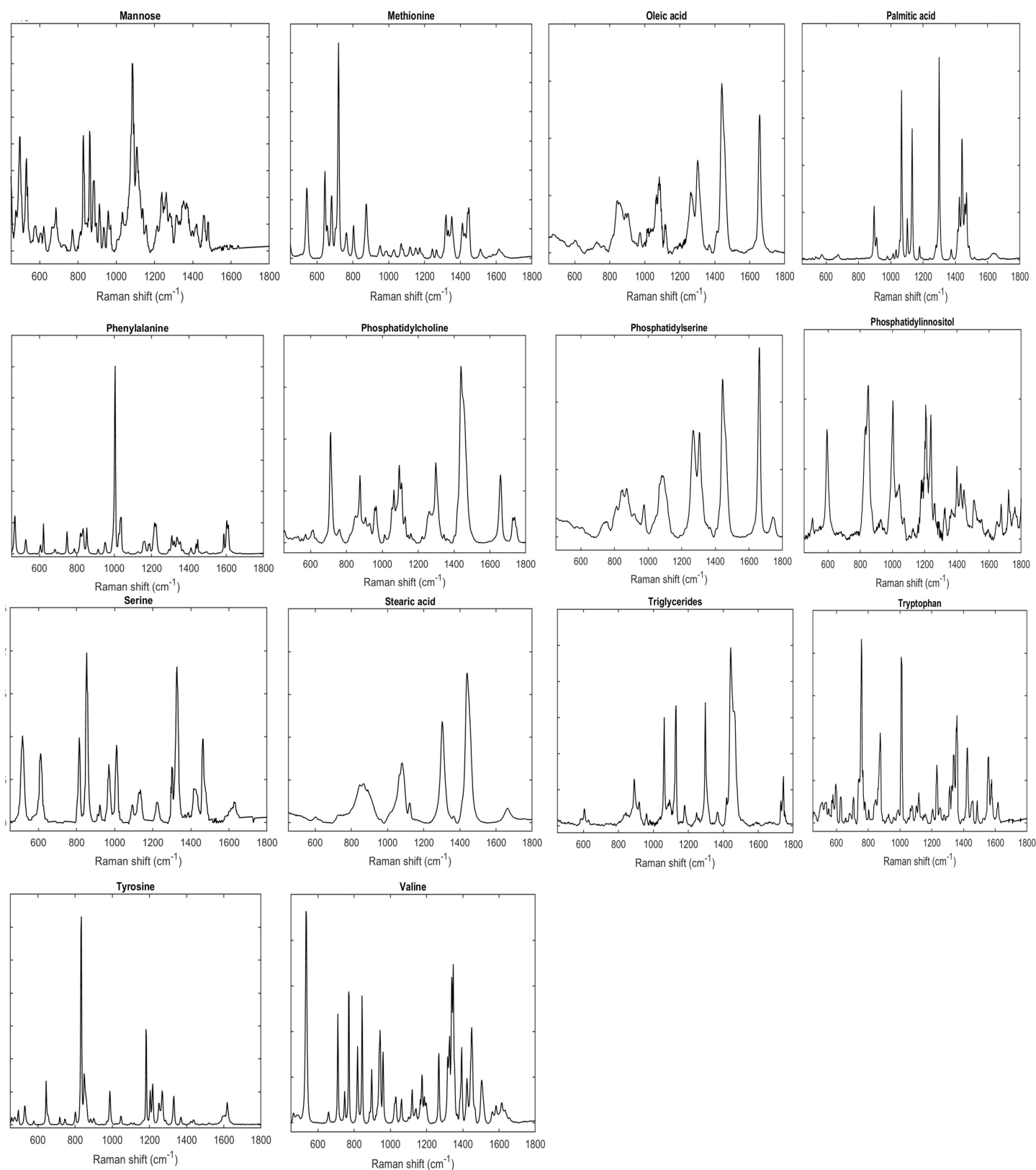


Figure S2. Raman spectra of biochemicals 17-30 as listed in table S1 which were used in the GBR-NMF model. All spectra were acquired using a Renishaw InVia system (dry 100x objective), using an excitation wavelength of 785 nm. Spectra were collected from biochemicals in their pure form. All spectra have been baseline corrected and smoothed using standard Savitsky-Golay filtering algorithms in MatLab. The spectra were then normalised such that the area under the curve was equal to 1.

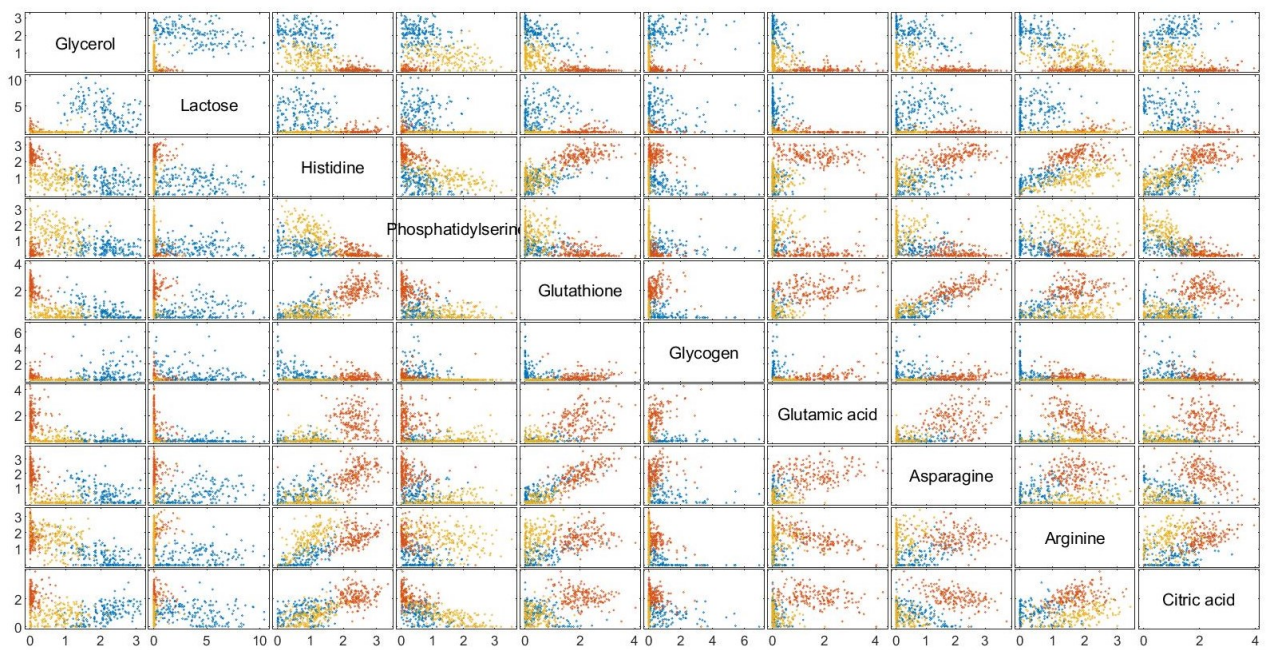


Figure S3. Scatter plot depicting scores of unirradiated controls for each cell line H460 (blue), MCF7 (red) and LNCaP (yellow) on the 10 most important chemicals obtained from random forest decision modelling, as labelled in the diagonal.

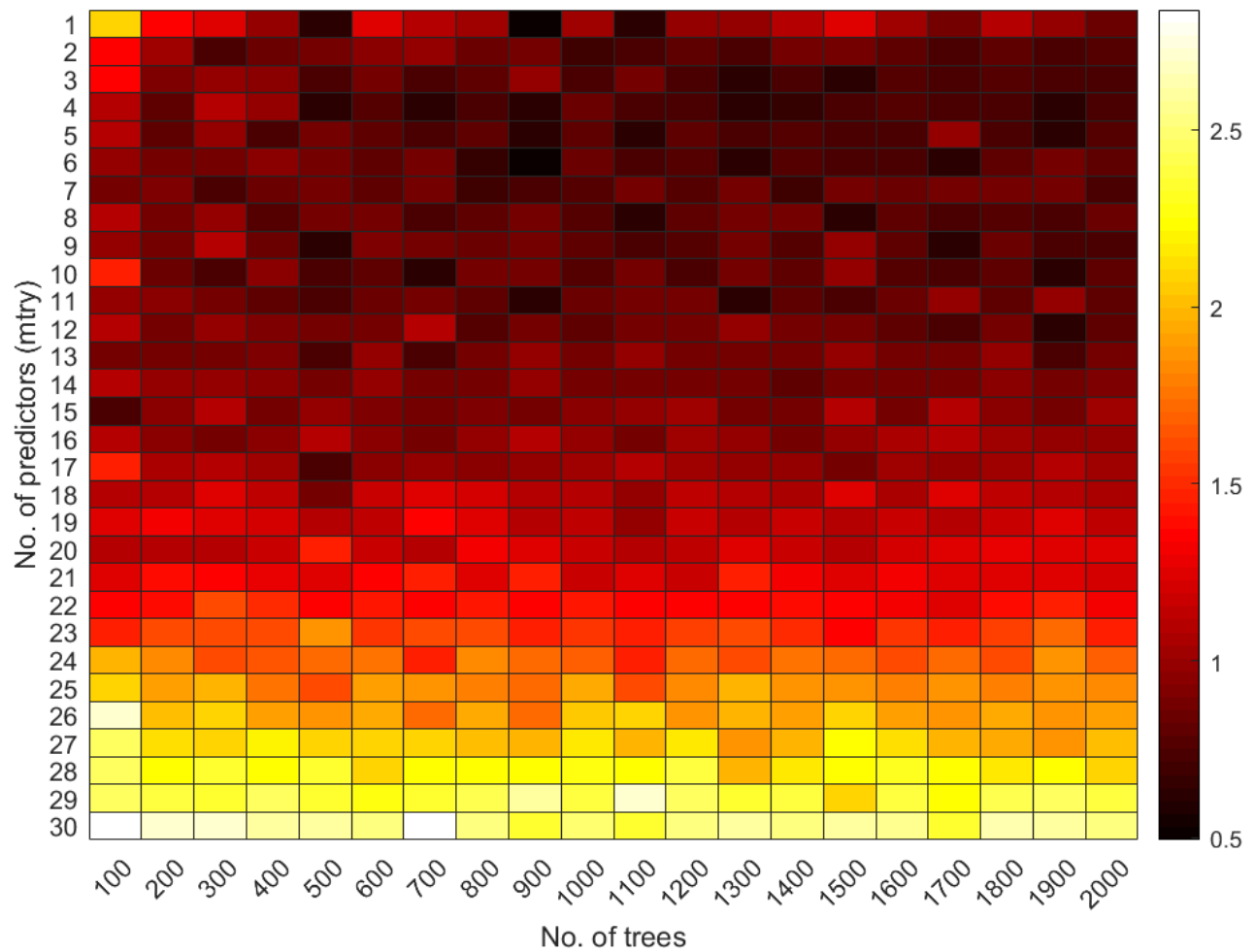


Figure S4. Heat map depicting OOB error as a misclassification percentage (average of 5 RF models) using various combinations of number of trees used in RF modelling (ranging from 100-2000 in increments of 100) and number of variables used to split each node (ranging from 1-30 in increments of 1) White pixels represent an error of 2.8% and deep red pixels represent an error of 0.5%. Colour bar depicts range in OOB error as a misclassification percentage. Heat map was generated using freely available software in Matlab version 2019b.